Baryon junction loops and the baryon-meson anomaly at high energies

V. Topor Pop,[1] M. Gyulassy,[2] J. Barrette,[1] C. Gale,[1] X. N. Wang,[3] and N. Xu[3]
[1]*McGill, University, Montreal, Canada, H3A 2T8*
[2]*Physics Department, Columbia University, New York, New York 10027, USA*
[3]*Nuclear Science Division, Lawrence Berkeley National Laboratory, Berkeley, California 94720, USA*
(Received 27 July 2004; published 21 December 2004)

A new version, v2.0, of the HIJING/$B\overline{B}$ Monte Carlo nuclear collision event generator is introduced in order to explore further the possible role of baryon junctions loops in the baryon-meson anomaly $(2 < p_T < 5\ \mathrm{GeV}/c)$ observed in $200A$ GeV Au+Au reactions at RHIC. We show that junction loops with an enhanced intrinsic $k_T \approx 1\ \mathrm{GeV}/c$ transverse momentum kick may provide a partial explanation of the anomaly as well as other important baryon stopping observables.

DOI: 10.1103/PhysRevC.70.064906 PACS number(s): 25.75.Dw, 25.75.Ld

I. INTRODUCTION

The phase transition from partonic degrees of freedom (quarks and gluons) in ultrarelativistic nuclear collisions to hadronic degree of freedom is a central focus of recent experiments at RHIC [1–6]. One of the interesting and unexpected discoveries [7,8] at RHIC is the "baryon anomaly" [9], observed as a large enhancement of the baryon to meson ratio and as a large difference between the nuclear modification factor $R_{AA}(p_T)$ between total charged and π^0 at moderate $2 < p_T < 5\ \mathrm{GeV}/c$. There are two main effects that contribute to this anomaly. One is the predicted jet quenching [9,10] that strongly suppresses the pion yield above $p_T > 2\ \mathrm{GeV}/c$. This effect causes an apparent enhancement since the pion denominator is reduced. The second effect is a genuine enhancement of baryon transverse momentum spectra. Several effects can contribute to such enhancements of baryon yields at moderate p_T. Radial hydrodynamical flow has been observed at all energies including RHIC [11]. However, at high p_T local equilibrium must fail. At intermediate p_T a nonequilibrium remnant of hydrodynamic flow may arise from multiquark recombination [6,12–15].

In this work we continue to explore the possibility that a more novel and unconventional source of baryon production may be at least partially responsible for the baryon anomaly. We study whether baryon junction loops, as proposed in Ref. [16] to explain (anti)hyperon production at lower (SPS) energies, could help explain the RHIC data. The idea that nonperturbative three-color flux junctions could play an important role in baryon and antibaryon production at high energies was proposed long ago by Rossi and Veneziano [17,18] on the basis of dual Regge theory. This idea was extended and applied by Kharzeev [19] to nuclear collisions. The first full $A+A$ event Monte Carlo implementation of this mechanism was the HIJING/B generator by Vance *et al.* [20]. The addition of the baryon junction loop mechanism led to the HIJING/$B\overline{B}$ 1.10 version of this model [16]. Unlike conventional diquark fragmentation models, a baryon junction allows the diquark to split with the three independent flux lines tied together at a junction. For an alternate possible formulation of baryon junction dynamics see Refs. [21–24].

In this paper we introduce a new version (v2.0) of HIJING/$B\overline{B}$ generator that differs from HIJING/$B\overline{B}$ v1.10 [16] in its implementation of hypothesized junction antijunction loops that may be responsible for novel baryon pair production in nucleus nucleus $(A+B)$ collisions. A large database on meson and baryon spectra [7,8,25–43] are now available from RHIC experiments. The HIJING event generator [44] was developed to extrapolate hadron-hadron multiparticle soft plus hard phenomenology as encoded in the LUND JETSET/PYTHIA model [45] to nuclear collisions. One important feature of HIJING is that it can account for the pion quenching component of the baryon anomaly. However, the LUND JETSET diquark string fragmentation mechanism used in HIJING v1.37 [44] completely fails to describe the baryon spectra observed in $A+A$ collisions at all energies [46–48]. HIJING/$B\overline{B}$ v1.10 was developed to address this failure at SPS energies. It was, however, also found to be inadequate, as we review below, with respect to baryon observables. For a recent discussion comparing HIJING v1.37 and HIJING/$B\overline{B}$ v1.10 predictions for global observables at RHIC see Ref. [48].

Clarifying the physical origin of the (anti-) baryon dynamics at RHIC is important given the variety of hadronization mechanisms proposed in hydrodynamic models [49], multiquark coalescence [12–15], thermal [50], hadron-string-dynamics (HSD) transport models [51] and the novel baryon junction dynamics [9,52]. The valence baryon number migration over the large rapidity window $-5 < y < 5$ at RHIC provides another stringent tests of the baryon dynamics. Recent RHIC data show at midrapidity a sizeable finite net-proton $(p\text{-}\overline{p})$ number in the final state [7,8,25–27,31–43]. Moreover, the antibaryon-to-baryon ratios are not equal to one, providing further evidence for non-transparency of high energy nuclei. This significant baryon number transport over more than 5 units in rapidity has inspired other approaches as well [53–57]. The net baryon density at midrapidity also has an impact on the hadrochemical equilibration affecting hadronic yields [58].

Another possible source of novel baryon-hyperon physics are strong color electric fields (SCF). This is modeled as an increase of the effective string tension that controls the $q\overline{q}$ and $qq\overline{q}\overline{q}$ pair creation rates [59,60]. A molecular dynamics model [61–64] have been used to study the effects of color ropes as an effective description of the non-perturbative, soft gluonic part of QCD [65–67]. SCF increases the parton "in-

 ©2004 The American Physical Society

trinsic transverse momentum" (k_T) and decreases the proton and antiproton yields. The empirical value of the Regge slope for baryon is $\alpha' \simeq 1$ GeV^{-2}, which yields a string tension κ (related to the Regge slope, $\kappa = 1/2\pi\alpha'$), of approximately 1 GeV/fm. It has been suggested that the magnitude of a typical field strength at RHIC energies might reach 5–12 GeV/fm [68]. However, in this work we will not consider further the consequences of SCF effects but concentrate only on the junction loops.

In the following sections we compare numerical results of HIJING/$B\bar{B}$ v2.0 to transverse momentum spectra, rapidity densities (dN/dy) of protons (p), antiprotons ($\bar{p}$), and netprotons (p-$\bar{p}$) for central Au+Au collisions at $\sqrt{s_{NN}}=200$ GeV as well as their centrality dependence. The characteristic stopping observables, average rapidity loss, energy loss of net-baryons per participant nucleon, and transverse energy per net baryons, are presented. The "anomalous" baryon-meson composition at moderate p_T observed in particle ratios $\bar{p}/p$, p/π^+, $\bar{p}/\pi^-$ and in species-dependent nuclear modification factors is also discussed.

In Sec. II we briefly recall the ingredients of the HIJING [44] and HIJING/$B\bar{B}$ (v1.10) [20,16] approaches and point out the extensions incorporated in the new version HIJING/$B\bar{B}$ v2.0. In Sec. III numerical results are discussed in detail in comparison with available data. A summary and conclusions are presented in Sec. IV.

II. HIJING/$B\bar{B}$ v2.0

HIJING is a model that provides a theoretical framework to extrapolate elementary proton-proton multiparticle phenomena to complex nuclear collisions as well as to explore possible new physics such as energy loss and gluon shadowing [56]. Three versions of this model will be compared in this paper: HIJING v1.37, HIJING/$B\bar{B}$ v1.10, and HIJING/$B\bar{B}$ v2.0. Detailed descriptions of the HIJING v1.37 and HIJING/$B\bar{B}$ v1.10 models can be found in Refs. [16,20,44,48].

In HIJING v1.37 [44] the soft beam jet fragmentation is modeled by diquark-quark strings as in Ref. [45] with gluon kinks induced by soft gluon radiations. The minijet physics is computed via an eikonal multiple collision framework using perturbative (PQCD) PYTHIA v5.3 to compute the initial and final state radiation and hard scattering rates. The cross section for hard parton scatterings is enhanced by a factor $K = 2$ in order to simulate high-order corrections. HIJING extends PYTHIA to include a number of new nuclear effects. Besides the Glauber nuclear eikonal extension, shadowing of nuclear parton distributions is modeled. In addition, dynamical energy loss of the (mini)jets is taken into account through an effective dE/dx.

In HIJING/$B\bar{B}$ v1.10 [16] the baryon junction mechanism was introduced as an extension of HIJING/B [20] in order to try to account for the observed longitudinal distributions of baryons (B) and antibaryons (B) in proton nucleus ($p+A$) and nucleus-nucleus ($A+A$) collisions at the SPS energies. However, as implemented in HIJING/$B\bar{B}$ v1.10 the junction loops fails to account for the observed enhanced transverse slopes of anti-baryons at moderate p_T in $A+A$ as shown in Ref. [48].

This is due to the limitations of p_T algorithm adopted in version 1.1 with kinematic constraints that worked to oppose the theoretically motivated junction $\sqrt{3}$ enhancement of the baryon junction loop p_T's [18,19]. In version 2.0 we therefore replaced that algorithm with one that implements a specified junction loop p_T enhancement directly. This is done by specifying the intrinsic (anti)diquark p_T kick in any standard (qq-q) string that contains one or multiple ($J\bar{J}$) loops. In addition, we have a new formula [see Eq. (1) below] for generating the probability that a given diquark or antidiquark gets an "enhanced p_T kick" from the underlying junction mechanism. We emphasize that while there is very strong evidence from a variety of data that the source of the observed baryon p_T enhancement may arise more naturally from collective hydrodynamic flow [49,69], elliptic flow of heavy hyperons [70] in particular argues most strongly for much of the partonic collective flow origin of the baryon anomaly. Nevertheless, our purpose here is to explore more fully, without the kinematic limitations of version 1.1, the theoretical problem of how much of the baryon anomaly at RHIC could be due to the long postulated baryon junction dynamics. Most of the initial baryon radial p_T could theoretically arise from the production mechanism, while its elliptic deformation would arise from final state interactions. We note, however, that in the latest study [14] of local dynamical (versus static global [13]) coalescence of baryons, the coalescence mechanism still cannot fully explain the observed 3-to-2 ratio for baryon to meson ellictic flow $[v_2(p_T), p_T > 2$ GeV$/c]$. The details of this new implementation of $J\bar{J}$ loops are described below.

Multiple hard and soft interactions proceed as in HIJING v1.37. Before fragmentation via JETSET, however, we compute the probability that a junction loop occurs in the string. A picture of a juction loop is as follows: a color flux line splits at some intermediate point into two-flux line at one junction, and then the flux line fuses back into one at a second anti-junction somewhere further along the original flux line. The distance in rapidity between these points is chosen via a Regge distribution as described below. For single inclusive baryon observables this distribution does not need to be specified.

The probability of such a loop is assumed to increase with the number of binary interactions, n_{hits}, that the incident baryon suffers in passing through the oncoming nucleus. This number depends on the relative and absolute impact parameters and is computed in HIJING using the eikonal path through a diffuse nuclear density.

We assume as in Ref. [16] that out of the nonsingle diffractive NN interaction cross section, $\sigma_{in} - \sigma_{nsd}$, a fraction $f_{J\bar{J}} = \sigma_{J\bar{J}}/(\sigma_{in} - \sigma_{nsd})$ of the events excite a junction loop. The probability after n_{hits} that the incident baryon has a $J\bar{J}$ loop is

$$P_{J\bar{J}} = 1 - (1 - f_{J\bar{J}})^{n_{hits}}. \quad (1)$$

We take $\sigma_{J\bar{J}} = 17$ mb, $\sigma_{sdf} \approx 10$ mb, and the total inelastic nucleon nucleon cross section $\sigma_{in} \approx 42$ mb at RHIC energies. These cross sections imply that a junction loop occurs in pp collisions at RHIC energy with a rather high probability $17/32 \approx 0.5$ and rapidly approaches 1 in AA. In p+S where

$n_{hit} \approx 2$ there is an 80% probability that a junction loop occurs in this scheme. Thus the effects of loops is taken here to have a very rapid onset and essentially all participant baryons are excited with $J\bar{J}$ loops in AA at RHIC. We investigate the sensitivity of the results to the value of parameter $\sigma_{J\bar{J}}$ and found no significant variation on pseudorapidity distributions of charged particles, for 15 mb $< \sigma_{J\bar{J}} <$ 25 mb for Au+Au. Light ion reactions like p+S and p+Ar would have more sensitivity to $\sigma_{J\bar{J}}$.

The production of a baryon and antibaryon from a $J\bar{J}$ loop is simulated via an enhancement of the diquark p_T kick parameter σ_{qq}=PARJ(21) of JETSET v7.3. The default value is σ_{qq}=0.36 GeV/c in ordinary string fragmentation. However in events where the string has a junction loop we can expect a significantly higher p_T kick [16]. We therefore propose a very simple algorithm whereby the $J\bar{J}$ is modeled by enhancing σ_{qq} by a factor F_{p_T}, which we fit to best reproduce the observed p_T spectrum of the baryons. This implementation of the $J\bar{J}$ model marks a radical departure from that implemented in HIJING/$B\bar{B}$ v1.10.

While the above model allows the baryon-antibaryon pairs to acquire much high transverse momentum in accord with observation, the absolute production rate also depends on the diquark-quark suppression factor PARJ(1). The JETSET default for ordinary (fundamental flux) strings has PARJ(1)=0.1. The reduced number of protons and antiprotons observed at RHIC relative to HIJING v1.37 will be shown below to be accounted for, if PARJ(1) is reduced to 0.07 in $J\bar{J}$ loops.

In summary, two paramters, PARJ(1), PARJ(21), are used in version 2.0 to *simulate* the dynamical consequences of the hypothesized $J\bar{J}$ loop production in $A+B$ reactions. The factor F_{p_T} modifying the default 0.36 GeV value of PARJ(21) may depend on beam energy, atomic mass number (A), and centrality (impact parameter). However, we will show that a surprisingly good description of a variety of observables is obtained with a constant value, $F_{p_T}=3$. The sensitivity of the theoretical predictions to this parameter is discussed in Sec. III.

Finally, we remark that correlations studies in $p+p$ and $p(d)$+Au collisions at RHIC energies could eventually help us to obtain more precise values of $J\bar{J}$ loop parameters [mainly $\sigma_{J\bar{J}}$, Regge intercept $\alpha_J(0)$, and F_{p_T}]. The contribution to the double differential inclusive cross section for the inclusive production of a B and $\bar{B}$ in NN collisions due to $J\bar{J}$ exchange is [16,19]

$$E_B E_{\bar{B}} \frac{d^6\sigma}{d^3p_B d^3p_{\bar{B}}} \to C_{B\bar{B}} e^{[\alpha_J(0)-1]|y_B - y_{\bar{B}}|}, \tag{2}$$

where $C_{B\bar{B}}$ is an unknown function of the transverse momentum and M_0^J+P+B (junction+Pomeron+baryon) couplings [16,20]. The predicted rapidity correlation length $[1-\alpha_J(0)]^{-1}$ depends upon the value of the intercept $\alpha_J(0)$. To test for the M_0^J component $\alpha_J(0) \simeq 0.5$ requires the measurement of rapidity correlations on a scale $|y_B - y_{\bar{B}}| \sim 2$. In contrast, infinite range rapidity correlations are suggested if $\alpha_J(0) \simeq 1.0$ [23]. It is thus important to look for rapidity correlations at RHIC energies where very high statistics data are now available, in $p+p \to B+\bar{B}+X$, or $p(d)+A \to B+\bar{B}+X$.

III. NUMERICAL RESULTS

A. Transverse momentum spectrum

The nuclear modification factor (R_{AA}) is defined as the ratio of the hadron yield in central Au+Au collisions to that in $p+p$ reactions scaled by the number of binary collisions (N_{coll}):

$$R_{AA}(p_\perp) = \frac{d^2N_{AA}/dydp_\perp}{\langle N_{coll}\rangle d^2N_{pp}/dydp_\perp}, \tag{3}$$

where $\langle N_{coll}\rangle$ is the average number of binary collisions of the event sample calculated from the nuclear overlap integral (T_{AA}) and the inelastic nucleon-nucleon cross section; $\langle N_{coll}\rangle = \sigma_{nn}^{inel}\langle T_{AA}\rangle$.

In Fig. 1 the measured [71] nuclear modification factor (R_{AA}) for charged hadrons in central (0–10 %) Au+Au collisons at 200 GeV are compared to the predictions of HIJING v1.37 and HIJING/$B\bar{B}$ v2.0 models. The data show the strong jet quenching effect that suppresses the hadrons yield by a factor of ≈ 5 for the highest p_T bins resulting in an observed maximum in R_{AA} at $p_T \approx 2$ GeV/c. Note that both *HIJING* v1.37 and HIJING/$B\bar{B}$ v1.10 fail to reproduce the "baryon bump" at moderate p_T seen in the R_{AA} factor and also fail to account for the large transverse slopes of baryons and antibaryons (see Ref. [48]). The Lund string fragmentation mechanism of hadronization in HIJING v1.37 leads to a rather slow increase of the nuclear modification factor R_{AA} to unity at high p_T, not observed in the data [see (a), results without quenching and shadowing effects (nqs)]. The addition of jet quenching and shadowing effects (yqs) in HIJING v1.37 still fails to describe the data.

In contrast, HIJING/$B\bar{B}$ v2.0 with shadowing and jet quenching (yqs) effects with default energy loss parameter dE/dx=1 GeV/fm (for the quark jet) describes well the data over the full p_T range. Some of the observed discrepancies could be attributed to strange and multistrange hyperons that are underestimated in our calculations because we do not consider SCF effects here.

Figure 2 presents a comparison of the experimental transverse mass distributions [25] of positive (left) and negative (right) particles with the predictions of HIJING/$B\bar{B}$ v2.0 (upper panel) and HIJING v1.37 (lower panel). The data shows a mass dependence in the shape of the spectra. The proton (p) and antiproton $(\bar{p})$ spectra have a shoulder-arm shape at low p_T characteristic of a radial flow. The pion spectra are well described by both models. Introducing the corrected $J\bar{J}$ loop algorithm in HIJING/$B\bar{B}$ v2.0 results in a significant improvement in the description of the protons and antiprotons in the scenario with shadowing and jet quenching. However, only a qualitative description is obtained for low $m_T - m_0$ spectra due to the presence of radial flow, not included in the model. A similar conclusion can be drawn from the predictions of the models for mean transverse momenta.

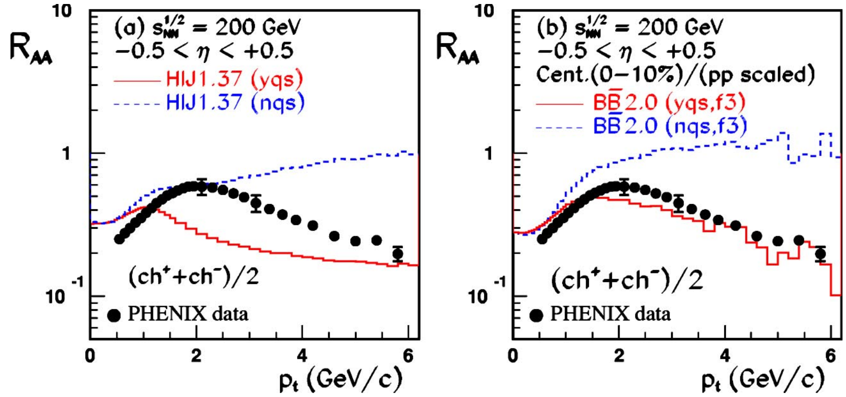

FIG. 1. (Color online) Comparison of HIJING v1.37 (left part) and HIJING/$B\overline{B}$ v2.0 (right part) predictions for the nuclear modification factor (R_{AA}) for central (0–10 %) Au+Au collisions at $\sqrt{s_{NN}}$=200 GeV. The results are with (solid histograms, yqs) or without (dashed histograms, nqs) shadowing and quenching effects included. The label f3 stands for model calculations assuming F_{p_T}=3. The data are from PHENIX [71]. Only statistical error bars are shown. The error bars at p_T=2 GeV and p_T=3 GeV, include systematic uncertainties. Equivalent error bars on the other points have been omitted for clarity.

Whereas the pion transverse momentum spectrum are rather well described at highest RHIC energies, there are still difficulties with the dynamics in the direction transverse to the beam for strange particles. Figure 3 presents a comparison of the experimental transverse mass distributions of positive [25] and neutral [28,29] kaons (upper part) as well as Λ (lower part) particles [28,29] with the predictions of HIJING v1.37 and HIJING/$B\overline{B}$ v2.0. The transverse momentum slopes of kaons-antikaons and Λ particles are underestimated in a scenario with shadowing and jet quenching (yqs). This failure points towards a dynamical origin that is not included in our present model and could be addressed by an explicit partonic interactions in a colored medium.

B. Stopping observables

Rapidity distributions of participants (net) baryons are very sensitive to the dynamical and statistical properties of nucleus-nucleus collisions. The RHIC net proton distribution is both qualitatively and quantitatively different from those at lower AGS and SPS energies [34]. Recent results for net protons in central (0–5 %) Au+Au interactions at a total

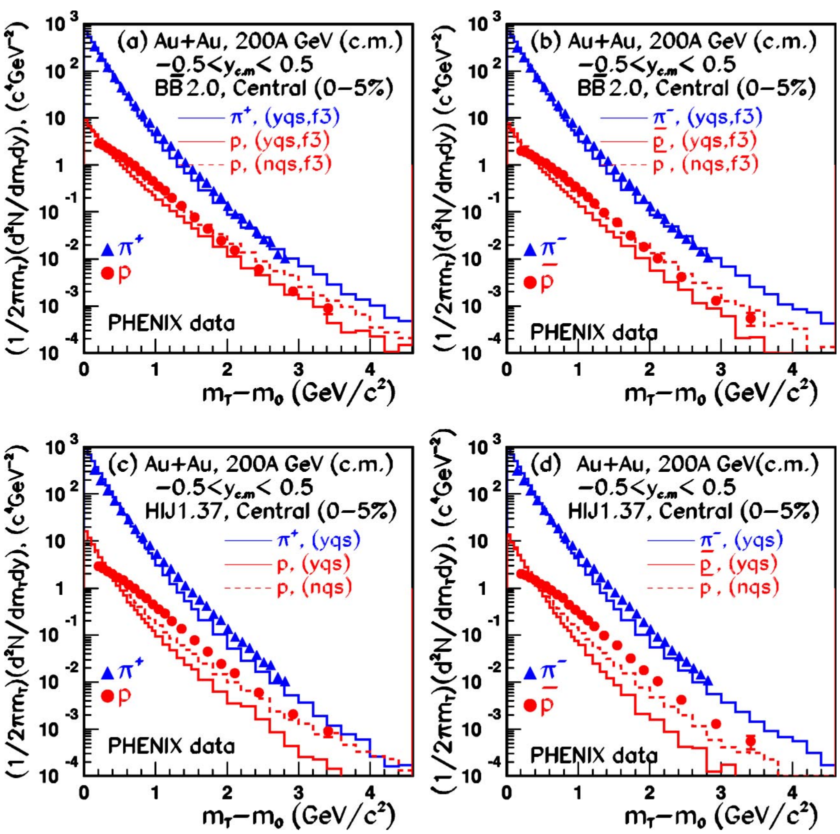

FIG. 2. (Color online) HIJING/$B\overline{B}$ v2.0 (upper panel) and HIJNG v1.37 (lower panel) predictions of transverse mass distributions for positive pions (π^+) and protons (p) (left part), and negative pions (π^-) and antiprotons ($\overline{p}$) (right part). The solid and dashed histograms have the same meaning as in Fig. 1. The data are from PHENIX [25]. The error bars show statistical errors only.

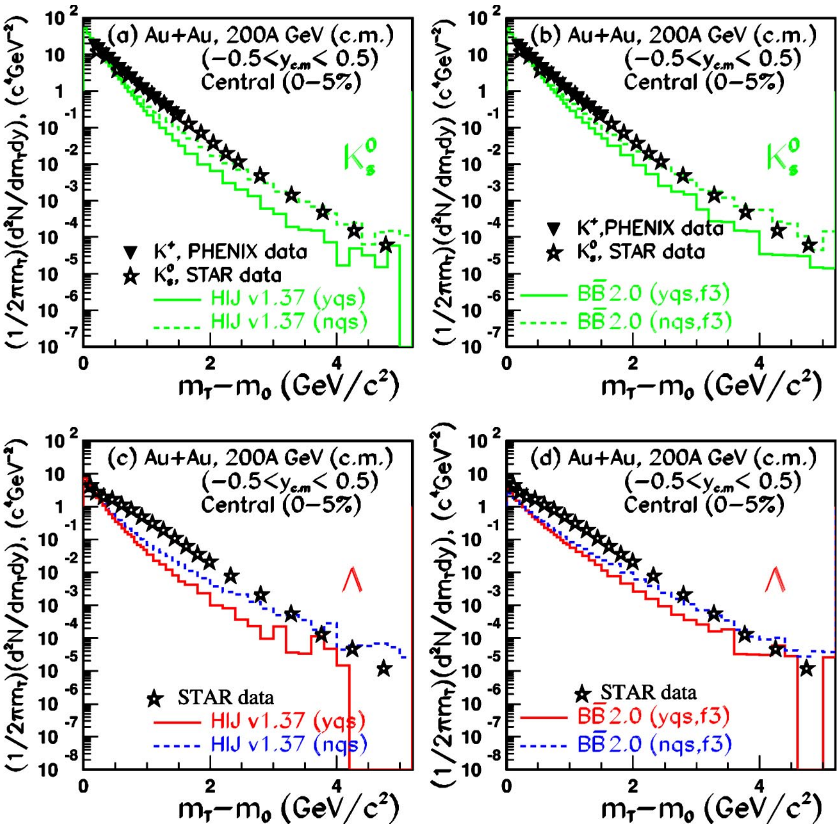

FIG. 3. (Color online) HIJNG v1.37 (left part) and HIJING/$B\overline{B}$ v2.0 (right part) predictions of transverse mass distributions for kaons (K^+, K_s^0 upper panel) and Λ particles (Λ, lower panel). The solid and dashed histograms have the same meaning as in Fig. 1. The data are K^+ from PHENIX [25] and K_s^0,Λ from STAR [28,29]. The error bars show statistical errors only.

nucleon nucleon center of mass (c.m.) energy $\sqrt{s_{NN}}$ =200 GeV show an unexpectedly large rapidity density at midrapidity [26,34].

Figure 4 presents a comparison of the rapidity distributions of protons [Fig. 4(a)], antiprotons [Fig. 4(b)] and net protons $(p\text{-}\overline{p})$ [Fig. 4(c)] and their ratio $(p/\overline{p})$ [Fig. 4(d)] obtained for Au+Au interactions at total c.m energy $\sqrt{s}$ =200*A* GeV with the model predictions of HIJING/$B\overline{B}$ v2.0 and RQMD v2.4 [60]. Corrections for feed-down contributions have been applied to the data. We discuss here a comparison with RQMD v2.4 results in order to investigate if hadronic rescattering only and SCF effects as implemented in RQMD, could explain the new data. The new version of HIJING/$B\overline{B}$ reproduces very well the experimental yield at midrapidity for both p and $\overline{p}$ as well as their ratio and the net proton yield $(p\text{-}\overline{p})$. This agreement is improved if shadowing and jet quenching are included. In contrast RQMD v2.4 does not reproduce the shape of the proton rapidity distribution near midrapidity and strongly underpredicts the antiproton yield.

In addition, the centrality dependence of proton and antiproton yields at midrapidity have been also analyzed and the results are shown in Fig. 5. HIJING/$B\overline{B}$ v1.0 overpredicts the data [26] except for very peripheral collisions. In contrast, HIJING/$B\overline{B}$ v2.0 reproduces very well the experimental yield at all centralities.

One of the main features of the data is the observed increase of net proton up to three units of rapidity away from midrapidity [Fig. 3(c)]. This central valley could be used as an indicator for partonic processes [72,73]. Microscopically, the baryon number transport over 4–5 units of rapidity to the equilibrated midrapidity region is not only due to hard processes acting on single valence (di)quark that are described by perturbative QCD, since this yields insufficient stopping [46,47]. Instead, additional processes such as the nonperturbative junction mechanism as implemented in HIJING/$B\overline{B}$ v2.0 are able to reproduce the observed distribution. Such a mechanism may lead to substantial stopping even at LHC energies.

The net-baryon $(B\text{-}\overline{B})$ distribution retains information about the energy loss and allows the degree of nuclear stopping to be determined. Experimentally, to obtain the net baryons, the number of net neutrons and net hyperons has to be estimated. In addition, the data need to be extrapolated to full rapidity space introducing other systematic errors. In contrast, in models we can calculate directly specific stopping observable as the average rapidity loss and the energy loss per participant nucleon as defined in Ref. [34]. The average rapidity loss is defined as $\langle \delta y\rangle = y_p - \langle y\rangle$, where y_p is the rapidity of the incoming projectile and $\langle y\rangle$ is the mean net-baryon rapidity after the collision

$$\langle y\rangle = \frac{2}{N_{part}}\int_0^{y_p} y\frac{dN_{(B-\overline{B})}}{dy}dy, \qquad (4)$$

where N_{part} is the number of participating nucleons in the collision.

The total energy E_{tot} per net baryon after the collisions can be derived using the relation

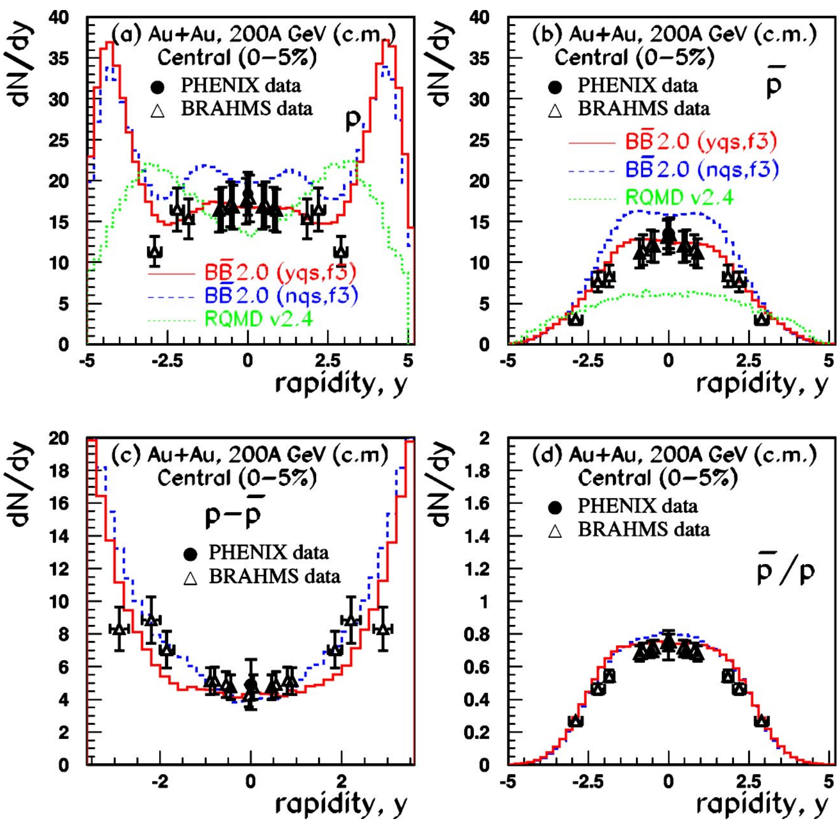

FIG. 4. (Color online) Calculated rapidity dependence of (a) protons, (b) antiprotons, (c) net protons, and (d) antiproton to proton ratio. The solid and dashed histograms have the same meaning as in Fig. 1. The dotted histograms correspond to RQMD v2.4 model predictions. The data, corrected for weak decays, are from PHENIX [26] and BRAHMS [34]. The errors bars shown includes both statistical and systematic uncertainties.

$$E_{tot} = \frac{1}{N_{part}} \int_{-y_p}^{y_p} \langle m_T \rangle \cosh y \frac{dN}{dy} dy, \tag{5}$$

where $\langle m_T \rangle = \langle \sqrt{p_T^2 + m_0^2} \rangle$ is the average transverse mass. The energy loss per participant pair could be estimated as $\Delta E = (100.0 - E_{tot})$ GeV. The predictions of the models for these quantities are presented in Fig. 6.

Figure 6(a) shows the net-baryon model predictions in comparison with BRAHMS data [34] obtained from the measured net proton ($N_{(B\text{-}\bar{B})} \approx 2N_{(p\text{-}\bar{p})}$). At RHIC energies a broad minimum has developed at midrapidity for net-baryon spanning few units of rapidity indicating that collisions are quite transparent. The average net-baryon rapidity loss deduced by BRAHMS $\langle \delta y \rangle = 2.0 \pm 0.2$ [34] is well reproduced by HIJING/$B\bar{B}$ v2.0. In contrast, the experimental value for the total energy per net baryon after the collisions, $E_{tot}^{exp} = 28 \pm 6$ GeV [34], are far from our theoretical predictions of both HIJING models, $E_{tot} \approx 40$ GeV.

The RQMD model [60] with rescattering and SCF effects strongly overpredicts the midrapidity net-baryon distributions and the average rapidity loss. Partly as a consequence E_{tot} per baryon after the collisions is underpredicted. The extrapolation to high rapidity used in Ref. [34] to obtain their values of $\langle \delta y \rangle$ and E_{tot} may explain part of the observed discrepencies. A precise measurement of transverse energy per baryon [as shown in Fig. 5(c)] could help also in the study concerning the origin of rescattering (which could influence the dynamics of the reaction at hadronic or partonic stage). However, futher analysis and baryon rapidity distribution measurements at large rapidity are needed in order to draw a final conclusion and to use these observables as a signature for partonic processes and for quark-guon plasma (QGP) formation.

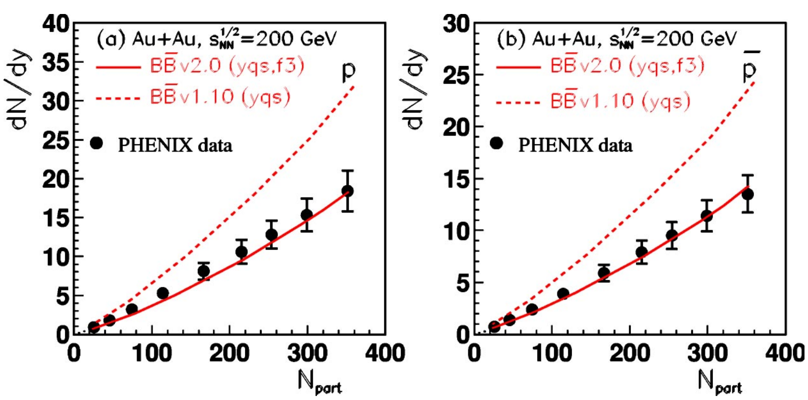

FIG. 5. (Color online) Comparison of HIJING/$B\bar{B}$ v1.10 (dashed lines) and HIJING/$B\bar{B}$ v2.0 (soild lines) predictions for the centrality dependence of proton (a) and antiproton (b) yields at midrapidity. The data are from PHENIX [26]. The errors shown includes both statistical and systematic uncertainties.

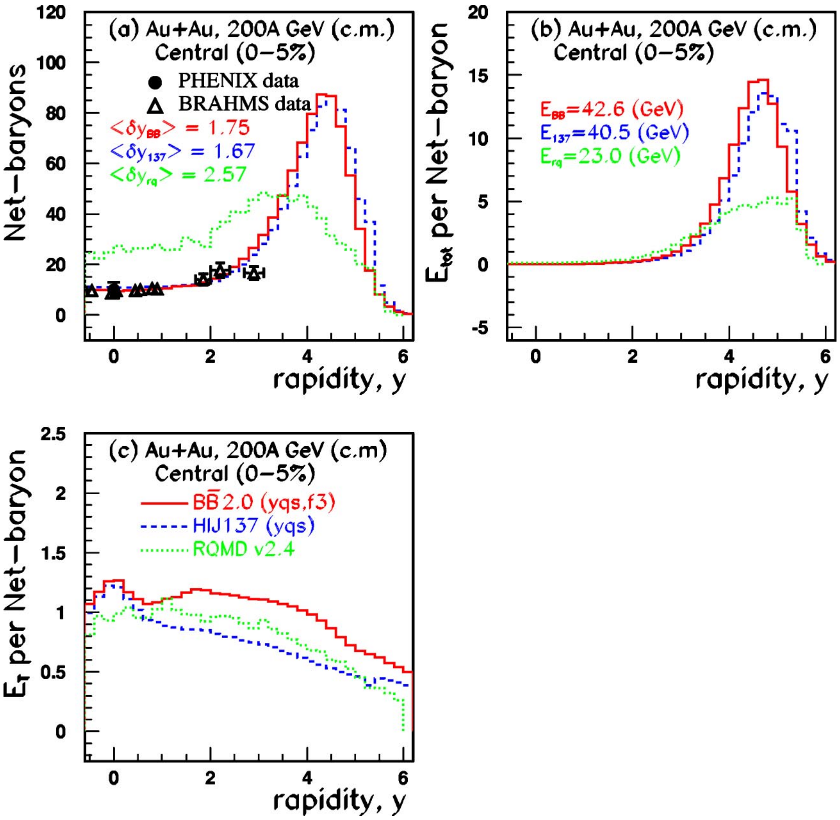

FIG. 6. (Color online) Model predictions for (a) the net-baryon distribution and the average rapidity loss $\langle \delta y \rangle$; (b) the total energy per netbaryon after the collisions; and (c) the transverse energy per net baryon for central (0–5 %) Au+Au collisions at $\sqrt{s_{NN}}$ =200 GeV. The solid and dashed histograms are the results obtained within HIJING/$B\overline{B}$ v2.0 and HIJING v1.37, respectively. The dotted histograms are the RQMD v2.4 predictions. The data are from BRAHMS [34]. The errors bars include both statistical and systematic uncertainties.

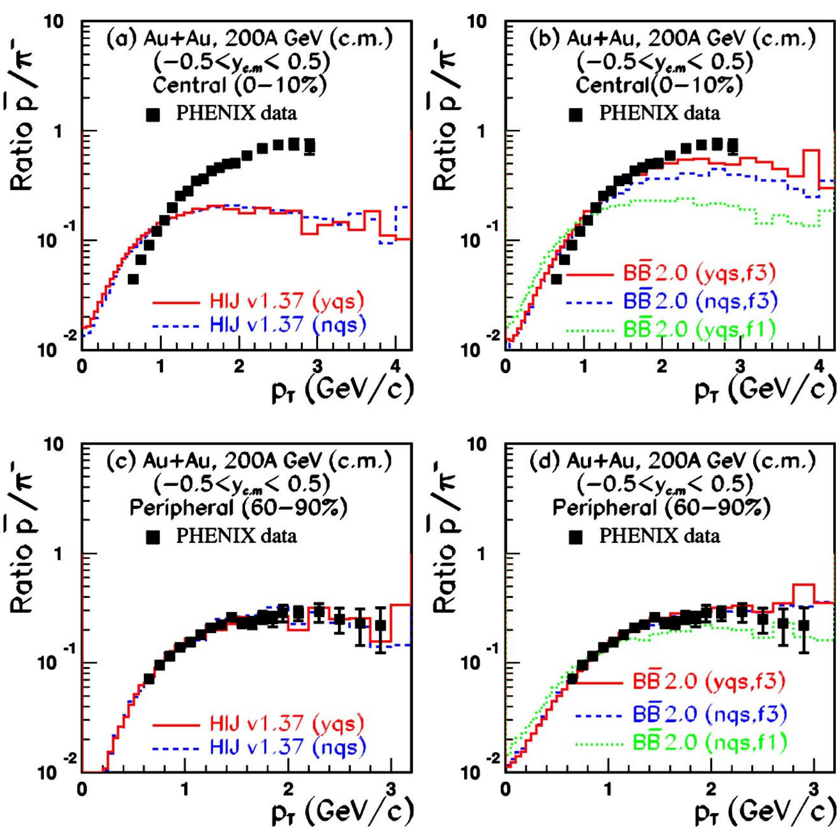

FIG. 7. (Color online) Model predictions for $\overline{p}/\pi^-$ ratio in central (0–10 %) Au+Au collisions at 200A GeV (upper part) and peripheral (60–90 %) Au+Au collisions (lower part). The solid and dashed histograms have the same meaning as in Fig. 1. In (b) and (d), the dotted histograms are the predictions of HIJING/$B\overline{B}$ v2.0 with F_{pT}=1 (label f1). The data are from PHENIX [26]. The error bars include systematic uncertainties.

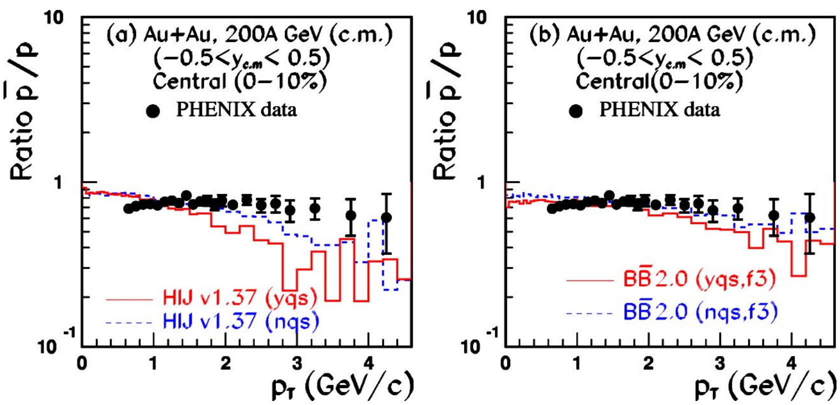

FIG. 8. (Color online) Comparison of HIJING v1.37 (left) and HIJING/$B\overline{B}$ v2.0 (right) model predictions for $\overline{p}/p$ ratio versus p_T for central (0–10 %) Au+Au collisions at 200*A* GeV. The solid and dashed histograms have the same meaning as in Fig. 1. The data are from PHENIX [26]. The error bars include systematic uncertainties.

C. Particle ratios versus p_T

In Fig. 7 the $\overline{p}/\pi^-$ ratio is shown as function of transverse momentum (p_T) for central (0–10 %) (upper part) and peripheral (60–90 %) collisions (lower part). The measured ratios increase at low p_T and saturate at different values that strongly increase from peripheral to central collisions. For central collisions at moderate p_T $(2<p_T<5\text{ GeV}/c)$, the yields of antiprotons $(\overline{p})$ are comparable to that of pions. In hard scattering processes described by PQCD and implemented in HIJING, the ratio $\overline{p}/\pi^-$ are determined by the fragmentation of energetic partons, independent of the initial colliding system. Therefore within the errors those ratios are well described for peripheral collisions by both version of the models. As expected in peripheral collisions there is little sensitivity to the new ingredients implemented in HIJING/$B\overline{B}$ v2.0. In contrast, the clear increase in the $\overline{p}/\pi^-$ ratio at moderate p_T from peripheral to central collisions is seen to be sensitive to the new physics as implemented in HIJING/$B\overline{B}$ v2.0. HIJING v1.37 strongly underpredicts the observed ratios at moderate p_T, an effect that is corrected in HIJING/$B\overline{B}$ v2.0, which includes an improved simulation of moderate p_T junction loop with a factor $F_{p_T}=3$.

A similar conclusion can be drawn from the results obtained for $\overline{p}/p$ ratio for central (0–10 %) Au+Au collisions at 200 GeV presented in Fig. 8 and for the p/π^+ ratio (not presented here). These results show the significant contributions of proton and antiproton yields to the total particle composition in this moderate p_T region $(2<p_T<5\text{ GeV}/c)$. An alternative interpretation of the observed increase with centrality is provided by the parton recombination and fragmentation model [12,13] while the hydrodynamics [49] and thermal model calculations predict that $\overline{p}/\pi^-$ ratio exceeds unity for central collisions.

In Fig. 9 the ratio Λ/K_s^0 is presented as function of transverse momentum (p_T) in comparison with HIJING v1.37 and HIJING/$B\overline{B}$ v2.0 model calculations. The data for Λ/K_s^0 ratio (hence baryon/meson) show a constant increase at low p_T to a plateau value of approximately 1.8 in central (0–5 %) collisions for moderate p_T $(2\leqslant p_T\leqslant 5\text{ GeV}/c)$. For central (0–5 %) and peripheral (60–90 %, not shown here) Au+Au collisions at moderate p_T, the ratio is underestimated within HIJING/$B\overline{B}$ v2.0 in both scenario with (yqs) and without (nqs) shadowing and quench effects. We note, that previous theoretical analysis which use various mechanism for baryon production such as recombinations [13] or HSD transport [51] underestimated also transverse momentum spectra for kaon-antikaon particles. In Ref. [51] this failure has been attributed to a lack of pressure generation in the very early phase of the heavy-ion collisions, which also shows up in the underestimation of the eliptic flow of charged hadrons at RHIC energies. This observation may be a signature of the strong color field effects [65,66].

D. Nuclear modification factor versus p_T

In order to better quantify the particle composition at moderate p_T we investigate the binary collision scaling of p_T spectra for charged pions, protons (antiprotons), and kaons (antikaons). Figure 10 shows the predicted nuclear modification factors R_{AA} and R_{cp} for the sum of protons and antipro-

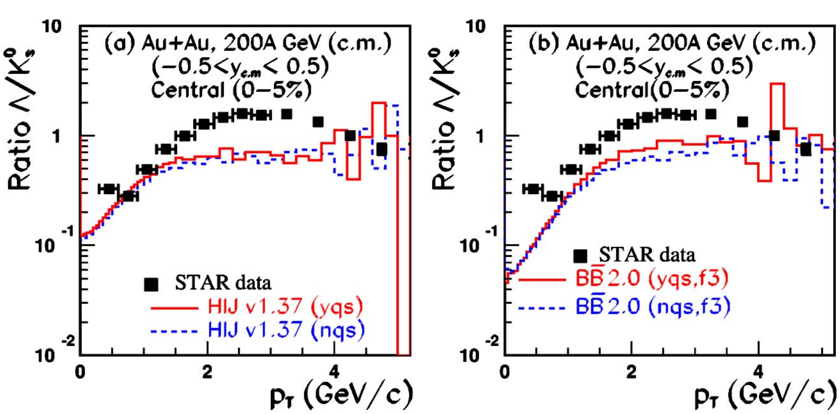

FIG. 9. (Color online) Comparison of HIJING v1.37 (left) and HIJING/$B\overline{B}$ v2.0 (right) model predictions for Λ/K_s^0 ratio versus p_T for central (0–5 %) Au+Au collisions at 200*A* GeV. The solid and dashed histograms have the same meaning as in Fig. 1. The data are from STAR [30]. The error bars bars show statistical errors only.

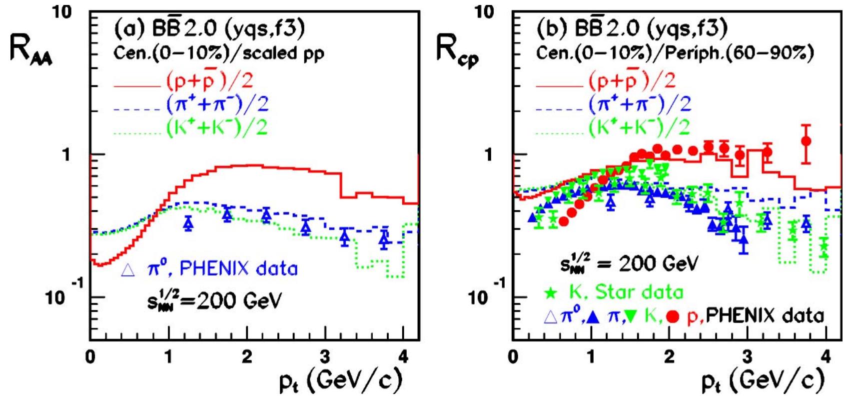

FIG. 10. (Color online) HIJING/$B\bar{B}$ v2.0 predictions for binary-collision scaled nuclear modification factor R_{AA} (a) and R_{cp} (b) for $(p+\bar{p})/2$ (solid histograms) charged pions (dashed histograms) and kaons (dotted histograms) in central (0–10 %) Au+Au collisions. The data are from PHENIX [26]. The K_S^0 data are from STAR [28,29] at slightly different centralities [central (0–5 %) and peripheral (60–80 %)]. The error bars are statistical only.

tons $(p+\bar{p})/2$, charged pions, and kaons in comparison with available PHENIX data [26].

R_{cp} is defined as the scaled yield ratio at different centrality such as the ratio of central to peripheral yield:

$$R_{cp}(p_\perp) = \frac{\text{Yield(central)}/\langle N_{coll}(\text{central})\rangle}{\text{Yield(periph.)}/\langle N_{coll}(\text{periph.})\rangle} \qquad (6)$$

where Yield$=(1/N_{events})(1/2\pi p_\perp)(d^2N/dp_\perp dy)$ and $\langle N_{coll}\rangle$ is defined as above.

The scaling behavior of the pions is different from those of the sum of protons and antiprotons. The pions yield scaled by N_{coll} in central events is strongly suppressed compared to pp reactions (R_{AA}) and to peripheral events (R_{cp}). The hadron production in HIJING/$B\bar{B}$ v2.0 is mainly from the fragmentation of energetic partons. Thus, the observed suppression in central collisions may be a signature of the energy loss of partons during their propagation through the hot and dense matter (possibly QGP) created in the collisions, i.e., *jet quenching*.

HIJING/$B\bar{B}$ v2.0 predicts that the sum of protons and antiprotons $(p+\bar{p})/2$ scales well with the number of binary collisions (N_{coll}). On the other hand, the discrepancy seen at $p_T < 1.5$ GeV/c indicates a sizable contribution from radial flow. Similar trend are observed in Λ, K_S^0 and $K^\pm$ measurements by the STAR Collaboration [28,29]. It has been recently shown that the competition between recombination and parton fragmentation at moderate p_T may also explain [12,13] the observed features.

IV. SUMMARY AND CONCLUSIONS

The failure of the previous implementation of baryon junction loops in HIJING/$B\bar{B}$ v1.10 to reproduce the observed p_T enhancement of antibaryons and baryons motivated us to construct a new version, HIJING/$B\bar{B}$ v2.0. The new physics ingredients implemented in HIJING/$B\bar{B}$ v2.0, concentrate on modifications of the hypothesized junction $J\bar{J}$ loops algorithm as well as adding a phenomenological simulation of collective transverse flow. These modifications make a significant improvement in the full event Monte Carlo description of a large set of observables for p and $\bar{p}$. The new version can account now for many features of the baryon anomaly region at moderate p_T, as well as for characteristic stopping observables at $\sqrt{s_{NN}}$=200 GeV in Au+Au collisions.

A simultaneous absence of suppression for baryons up to p_T=4–5 GeV/c and the enhancement of the p/π ratios at moderate p_T, which is a challenge for many theoretical frameworks, is well described within HIJING/$B\bar{B}$ v2.0 with shadowing and jet quenching effects, for an energy loss parameter dE/dx=1 GeV/fm (for quark jet) and a constant phenomenological factor F_{p_T}=3. One of the remaining discrepancies is the energy loss per participant nucleon and baryon rapidity measurements at forward rapidity ($y>3$), which will require futher analysis.

While this new version HIJING/$B\bar{B}$ v2.0 gives a good description of a large body of data it still cannot reproduce the transverse mass spectra of kaons and Λ particles for which the integrated yield is well predicted, but the model has no mechanism to account for radial flow of these particles. In string fragmentation phenomenology, the strong enhancement of strange particle observables require strong color field effects (SCF) [65,66]. The full understanding of the production of strange particles in relativistic heavy-ion collisions [51] remains an exciting open question.

ACKNOWLEDGMENTS

The authors would like to thank Subal Das Gupta for a careful reading of the manuscript and to thank Stephen Vance. One of us (V.T.P.) thanks Rene Bellwied and Mathew Lamont for helpful correspondence. This work was partly supported by the Natural Science and Engineering Research Council of Canada and the "*Fonds Nature et Technologies*" of Quebec. This work was supported also by the Director, Office of Energy Research, Office of High Energy and Nuclear Physics, Division of Nuclear Physics, and by the Office of Basic Energy Science, Division of Nuclear Science, of the U. S. Department of Energy under Contract Nos. DE-AC03-76SF00098 and DE-FG-02-93ER-40764.

[1] Proceedings of the 16th International Conference on Ultra-Relativistic Nucleus-Nucleus Collisions (QM02), Nantes, France, 2002, edited by H. Gutbrod, J. Aichelin, and K. Werner [Nucl. Phys. **A715**, 1c (2003)].
[2] Proceedings of 17th International Conference on Ultra-Relativistic Nucleus-Nucleus Collisions (QM04), Oakland, US, 2004, edited by H. G. Ritter and X.-N. Wang [J. Phys. G **30**, S633 (2004)].
[3] M. Gyulassy, Proceedings of NATO Advanced Study Institute: Structure and Dynamics of Elementary Matter, Kemer, 2003, edited by W. Greiner (to be published), nucl-th/0403032.
[4] "New Discoveries at RHIC—The Strongly Interactive QGP," Proceedings of RIKEN BNL Workshop, May, 2004, Brookhaven, N.Y.; RBRC Scientific Articles, **9**, 1 (2004).
[5] M. Gyulassy and L. McLerran, in Ref. [4], p. 23.
[6] B. Müller, in Ref. [4], p. 77.
[7] PHENIX Collaboration, K. Adcox *et al.*, Phys. Rev. Lett. **88**, 242301 (2002); **89**, 092302 (2002).
[8] PHENIX Collaboration, S. S. Adler *et al.*, Phys. Rev. Lett. **91**, 172301 (2003).
[9] I. Vitev and M. Gyulassy, Phys. Rev. C **65**, 041902 (2002); I. Vitev, M. Gyulassy and P. Levai, hep-ph/0109198 (2001).
[10] M. Gyulassy, I. Vitev, X.-N. Wang, and B.-W. Zhang, in *Quark Gluon Plasma 3*, edited by R. C. Hwa and X.-N. Wang (World Scientific, Singapore, 2003), pp. 123–191, and references therein.
[11] N. Xu and M. Kaneta, Nucl. Phys. **A698**, 306c (2002).
[12] Z. W. Lin and C. M. Ko, Phys. Rev. Lett. **89**, 202302 (2002); C. Nonaka, R. J. Fries, and S. A. Bass, Phys. Lett. B **583**, 73 (2004); C. Nonaka, B. Muller, M. Asakawa, S. A. Bass, and R. J. Fries, Phys. Rev. C **69**, 031902 (2004); R. C. Hwa and C. B. Yang, *ibid.* **67**, 034902 (2003); V. Greco, C. M. Ko, and P. Levai, Phys. Rev. Lett. **90**, 202302 (2003).
[13] R. J. Fries, B. Muller, C. Nonaka, and S. A. Bass, Phys. Rev. C **68**, 044902 (2003).
[14] D. Molnar, Acta Phys. Hung. New Ser.: Heavy Ion Phys. **A19**, 1 (2004).
[15] S. Pratt and S. Pal, nucl-th/0409038.
[16] S. E. Vance and M. Gyulassy, Phys. Rev. Lett. **83**, 1735 (1999). See http://www-cunuke.phys.columbia.edu/people/svance/hjbb.html. S. E. Vance, Ph.D. thesis, Columbia University (1999) [http://www-cunuke.phys.columbia.edu/people/svance/thesis.html].
[17] G. C. Rossi and G. Veneziano, Nucl. Phys. **B123**, 507 (1977).
[18] G. C. Rossi and G. Veneziano, Phys. Rep. **63**, 153 (1980).
[19] D. Kharzeev, Phys. Lett. B **378**, 238 (1996).
[20] S. E. Vance, M. Gyulassy, and X.-N. Wang, Phys. Lett. B **443**, 45 (1998).
[21] B. Z. Kopeliovich and B. G. Zakharov, Phys. Lett. B **211**, 221 (1988); Z. Phys. C **43**, 241 (1989).
[22] G. H. Arakelian, A. Capella, A. B. Kaidalov, and Yu. M. Shabelski, Eur. Phys. J. C **26**, 81 (2002).
[23] B. Kopeliovich and B. Povh, Phys. Lett. B **446**, 321 (1999).
[24] F. Bopp and Yu. M. Shabelski, hep-ph/0406158.
[25] PHENIX Collaboration, S. S. Adler *et al.*, Phys. Rev. C **69**, 034909 (2004).
[26] PHENIX Collaboration, K. Adcox *et al.*, Phys. Rev. C **69**, 024904 (2004).
[27] STAR Collaboration, J. Adams *et al.*, Phys. Rev. Lett. **92**, 112301 (2004).
[28] H. Long (for the STAR Collaboration), J. Phys. G **30**, S193 (2004).
[29] STAR Collaboration, J. Adams *et al.*, Phys. Rev. Lett. **92**, 052302 (2004).
[30] M. A. C. Lamont (for the STAR Collaboration), J. Phys. G **30**, S963 (2004).
[31] STAR Collaboration, J. Adams *et al.*, Phys. Rev. C **70**, 041901 (2004).
[32] STAR Collaboration, C. Adler *et al.*, Phys. Rev. Lett. **87**, 262302 (2001); **86**, 4778 (2001); **89**, 092301 (2002).
[33] BRAHMS Collaboration, D. Ouerdane *et al.*, J. Phys. G **30**, S1129 (2004).
[34] BRAHMS Collaboration, I. G. Bearden *et al.*, Phys. Rev. Lett. **93**, 102301 (2004).
[35] BRAHMS Collaboration, J. H. Lee, Nucl. Phys. **A715**, 482c (2003).
[36] BRAHMS Collaboration, I. G. Bearden *et al.*, Phys. Rev. Lett. **90**, 102301 (2003).
[37] BRAHMS Collaboration, P. Christiansen *et al.*, Nucl. Phys. **A721**, 239 (2003).
[38] BRAHMS Collaboration, I. G. Bearden *et al.*, Nucl. Phys. **A698**, 667c (2002).
[39] BRAHMS Collaboration, I. G. Bearden *et al.*, Phys. Rev. Lett. **87**, 112305 (2001).
[40] PHOBOS Collaboration, B. B. Back *et al.*, Phys. Rev. C **70**, 011901 (2004).
[41] PHOBOS Collaboration, B. Wosiek *et al.*, Nucl. Phys. **A715**, 510c (2003).
[42] PHOBOS Collaboration, B. B. Back *et al.*, Phys. Rev. C **67**, 021901 (2003).
[43] PHOBOS Collaboration, B. B. Back *et al.*, Phys. Rev. Lett. **87**, 102301 (2001).
[44] X.-N. Wang and M. Gyulassy, Phys. Rev. D **44**, 3501 (1992); **45**, 844 (1992); M. Gyulassy and X.-N. Wang, Comput. Phys. Commun. **83**, 307 (1994); X.-N. Wang, Phys. Rep. **280**, 287 (1997); X.-N. Wang, Nucl. Phys. **A661**, 609c (1999).
[45] T. Sjostrand, Comput. Phys. Commun. **82**, 74 (1994).
[46] V. Topor Pop, M. Gyulassy, X.-N. Wang, A. Andrighetto, M. Morando, F. Pellegrini, R. A. Ricci, and G. Segato, Phys. Rev. C **52**, 1618 (1995); M. Gyulassy, V. Topor Pop, and X.-N. Wang, *ibid.* **54**, 1498 (1996).
[47] M. Gyulassy, V. Topor Pop, and S. E. Vance, Heavy Ion Phys. **5**, 299 (1997).
[48] V. Topor Pop, M. Gyulassy, J. Barrette, C. Gale, X.-N. Wang, N. Xu, and K. Filimonov, Phys. Rev. C **68**, 054902 (2003).
[49] P. F. Kolb and U. Heinz, in *Quark Gluon Plasma 3*, edited by R. C. Hwa and X.-N. Wang (World Scientific, Singapore, 2003), pp. 634–714 and references therein; D. Teaney, J. Lauret, and E. V. Shuryak, Phys. Rev. Lett. **86**, 4783 (2001).
[50] P. Braun-Munzinger, D. Magestro, K. Redlich, and J. Stachel, Phys. Lett. B **518**, 41 (2001); F. Becatini *et al.*, Phys. Rev. C **64**, 024901 (2001); W. Florkowski, W. Broniowski, and M. Michalec, Acta Phys. Pol. B **33**, 761 (2002).
[51] E. L. Bratkovskaya, M. Bleicher, M. Reiter, S. Soff, H. Stocker, M. van Leeuwen, S. A. Bass, and W. Cassing, Phys. Rev. C **69**, 054907 (2004).
[52] T. Sjostrand and P. Z. Skands, J. High Energy Phys. **3**, 53 (2004).
[53] W. Busza and R. Ledoux, Annu. Rev. Nucl. Part. Sci. **38**, 119 (1988).

[54] H. Sorge, A. von Keitz, R. Mattiello, H. Stocker, and W. Greiner, Phys. Lett. B **243**, 7 (1990).
[55] L. Frankfurt and M. Strikman, Phys. Rev. Lett. **66**, 2289 (1991).
[56] X.-N. Wang and M. Gyulassy, Phys. Rev. Lett. **68**, 1480 (1992).
[57] A. Capella, Acta Phys. Pol. B **34**, 3331 (2003).
[58] P. Braun-Munzinger and J. Stachel, Phys. Lett. B **465**, 15 (1999).
[59] T. S. Biro, H. B. Nielsen, and J. Knoll, Nucl. Phys. **B245**, 449 (1984).
[60] H. Sorge, M. Berenguer, H. Stocker, and W. Greiner, Phys. Lett. B **289**, 6 (1992); H. Sorge, Phys. Rev. C **52**, 3291 (1995).
[61] S. Scherer, M. Hofmann, M. Bleicher, L. Neise, H. Stocker, and W. Greiner, New J. Phys. **3**, 8 (2001).
[62] M. Hofmann, S. Scherer, M. Bleicher, L. Neise, H. Stocker, and W. Greiner, Phys. Lett. B **478**, 161 (2000).
[63] S. Bass *et al.*, Prog. Part. Nucl. Phys. **41**, 255 (1998).
[64] M. Bleicher *et al.*, J. Phys. G **25**, 1859 (1999).
[65] S. Soff, J. Phys. G **30**, s139 (2004).
[66] S. Soff, J. Randrup, H. Stocker, and N. Xu, Phys. Lett. B **551**, 115 (2003).
[67] S. Soff, S. Kesavan, J. Randrup, H. Stocker, and N. Xu, Phys. Rev. Lett. (submitted). nucl-th/0404005.
[68] V. Magas, L. Csernai, and D. Strottman, Phys. Rev. C **64**, 014901 (2001).
[69] D. Kharzeev *et al.*, Nucl. Phys. B **119**, 13 (2003).
[70] J. Castillo (for the STAR Collaboration), J. Phys. G **30**, S181 (2004).
[71] PHENIX Collaboration, S. S. Adler *et al.*, Phys. Rev. C **69**, 034910 (2004).
[72] S. A. Bass, B. Muller, and D. K. Srivastava, Phys. Rev. Lett. **91**, 052302 (2003).
[73] G. Wolschin, Phys. Lett. B **569**, 67 (2003).